Structural Studies of Interactions between Cardiac Troponin I and Actin in Regulated Thin Filament Using Förster Resonance Energy Transfer[†]

Jun Xing,[‡] Mathivanan Chinnaraj,[‡] Zhihong Zhang,[§] Herbert C. Cheung,[‡] and Wen-Ji Dong*,[‖]

Department of Biochemistry and Molecular Genetics, University of Alabama at Birmingham, Birmingham, Alabama 354294, and Department of Pharmaceutical Sciences and The Voiland School of Chemical Engineering and Bioengineering and Department of Veterinary and Comparative Anatomy Pharmacology and Physiology, Washington State University, Pullman, Washington 99164

Received August 8, 2008; Revised Manuscript Received October 30, 2008

ABSTRACT: The Ca^{2+}-induced interaction between cardiac troponin I (cTnI) and actin plays a key role in the regulation of cardiac muscle contraction and relaxation. In this report we have investigated changes of this interaction in response to strong cross-bridge formation between myosin S1 and actin and PKA phosphorylation of cTnI within reconstituted thin filament. The interaction was monitored by measuring Förster resonance energy transfer (FRET) between the fluorescent donor 5-(iodoacetamidoethyl)aminonaphthalene-1-sulfonic acid (AEDANS) attached to the residues 131, 151, 160 167, 188, and 210 of cTnI and the nonfluorescent acceptor 4-(dimethylamino)phenylazophenyl-4′-maleimide (DABM) attached to cysteine 374 of actin. The FRET distance measurements showed that bound Ca^{2+} induced large increases in the distances from actin to the cTnI sites, indicating a Ca^{2+}-triggered separation of cTnI from actin. Strongly bound myosin S1 induced additional increases in these distances in the presence of bound Ca^{2+}. The two ligand-induced increases were independent of each other. These two-step changes in distances provide a direct link of structural changes at the interface between cTnI and actin to the three-state model of thin filament regulation of muscle contraction and relaxation. When cTnC was inactivated through mutations of key residues within the 12-residue Ca^{2+}-binding loop, strongly bound S1 alone induced increases in the distances in spite of the fact that the filaments no longer bound regulatory Ca^{2+}. These results suggest bound Ca^{2+} or strongly bound S1 alone can partially activate thin filament, but full activation requires both bound Ca^{2+} and strongly bound S1. The distributions of the FRET distances revealed different structural dynamics associated with different regions of cTnI in different biochemical states. The second actin-binding region appears more rigid than the inhibitory/regulatory region. In the Mg^{2+} state, the regulatory region appears more flexible than the inhibitory region, and in the Ca^{2+} state the inhibitory region becomes more flexible. PKA phosphorylation of cTnI at Ser23 and Ser24 distance from actin to cTnI residue 131 by 2.2−5.2 Å in different biochemical states and narrowed the distributions of the distances from actin to the inhibitory and regulatory regions of cTnI. The observed phosphorylation effects are likely due to an intramolecular interaction of the phosphorylated N-terminal segment and the inhibitory region of cTnI.

The Ca^{2+}-dependent interaction between cardiac troponin I (cTnI) and actin is one of the most important events in the regulation of cardiac muscle contraction and relaxation. We have investigated structural features of the interaction and how they are modulated by strong cross-bridge and PKA[1] phosphorylation of cTnI. Ca^{2+} regulation of myofilaments is linked to the thin filament, composed of the heterotrimeric troponin complex and tropomyosin (Tm) bound to the double helical actin filament (*1, 2*). In the cardiac myofilament troponin consists of troponin C (cTnC), cTnI, and troponin T (cTnT). In relaxed muscle, cTnI−Tm acting as a regulatory switch prevents cross-bridge formation between actin and the myosin subfragment-1 (S1) through steric blocking of myosin-binding sites on actin. To activate muscle, Ca^{2+} saturates the regulatory site of cTnC, triggering a series of conformational transitions among the thin filament proteins, including cTnI−actin interaction. These conformational changes ultimately result in strong force-generating interactions between myosin and actin (*3*). The Ca^{2+}-induced filament activation (structural transitions) is further modulated by the strong actin−myosin interaction and phosphorylation

[†] This work was supported in part by National Institutes of Health Grants HL80186 (W.-J.D.) and HL52508 (H.C.C.).

* Corresponding author. Tel: (509) 335-5798. Fax: (509) 335-3650. E-mail: wdong@vetmed.wsu.edu.

[‡] Department of Biochemistry and Molecular Genetics, University of Alabama at Birmingham.

[§] Department of Pharmaceutical Sciences, Washington State University.

[‖] The Voiland School of Chemical Engineering and Bioengineering, and Department of Veterinary and Comparative Anatomy Pharmacology and Physiology, Washington State University.

[1] Abbreviations: Tn, troponin; TnC, troponin C; TnI, troponin I; TnT, troponin T; Tm, tropomyosin; c, cardiac muscle; PKA, protein kinase A; FRET, Förster resonance energy transfer; DTT, dithiothreitol; Mops, 3-(*N*-mopholino)propanesulfonic acid; EGTA, ethylene glycol bis(β-aminoethyl ether)-*N*,*N*,*N*′,*N*′-tetraacetic acid; IAEDANS, 5-(iodoacetamidoethyl)aminonaphthalene-1-sulfonic acid; DABM, 4-(dimethylamino)phenylazophenyl-4′-maleimide.

10.1021/bi801492x CCC: $40.75
Published on Web 11/20/2008

of cTnI (*4*−*7*). This feedback activation of the thin filament is generally accepted to play a more prominent role in the activation of cardiac muscle than skeletal muscle for the beat-to-beat regulation of cardiac output. Despite extensive studies on functional effects, there is little information related to the molecular basis for the protein−protein interactions within the thin filament that underlie the feedback of strong cross-bridges and cTnI PKA phosphorylation on myofilament activation.

A main feature of regulation of cardiac muscle is the dynamics of the interaction among the thin filament proteins involving multiple structural transitions at the thin filament protein interfaces. This dynamics gives rise to a cooperativity of structural interactions and kinetic coupling of signaling steps during muscle activation. An important challenge in the study of cardiac thin filament regulation is to understand the significance of alterations at the molecular level, i.e., protein−protein interactions in response to signal transduction from Ca^{2+} binding to force generation. This information is essential to our understanding of how the actin−myosin interaction is activated and how this activation is modulated by cross-bridge formation and other mechanisms. In this report, we focused our investigation on structural changes in the interaction between the C-terminal region of cTnI and actin Cys374 in response to Ca^{2+} binding to troponin, strong cross-bridge formation, and cTnI PKA phosphorylation. The C-terminal region of cTnI contains several functional domains including the inhibitory region (residues 130−150), the regulatory region (residues 151−167), and the second or "mobile" actin-binding domain (residues 168−210). The interaction between the C-terminal region of cTnI and actin within the thin filament was monitored by measuring Förster resonance energy transfer (FRET) between the fluorescent 5-(iodoacetamidoethyl)aminonaphthalene-1-sulfonic acid (AEDANS) as donor attached to selected residues in the C-terminal region of cTnI and the nonfluorescent 4-(dimethylamino)phenylazophenyl-4′-maleimide (DABMI) as acceptor attached to cysteine 374 of actin. Our results provide quantitative information on a two-step movement of the inhibitory/regulatory region of cTnI (residues 130−167) from actin filament following Ca^{2+} activation and strong cross-bridge formation between myosin S1 and actin. This two-step transition is well correlated with the three-state model of thin filament activation. An analysis of the distribution of the measured FRET distances indicates that the structural dynamics of the inhibitory/regulatory region of cTnI is significantly altered upon phosphorylation of the N-terminal segment of cTnI by PKA at Ser23 and Ser24.

MATERIALS AND METHODS

Protein Preparations. A recombinant wild-type cTnT mutant was generated from a full-length rat cTnT clone subcloned into a pET-17b vector, and a recombinant wild-type cTnC was generated from a cTnC cDNA clone from chicken slow skeletal muscle as previously reported (*8*). cTnI mutants containing a single cysteine at positions 131 (C81I/C98S/Q131C), 151 (C81I/C98S/S151C), 160 (C81I/C98S/L160C), 167 (C81I/C98S/S167C), 188 (C81I/C98S/E188C), and 210 (C81I/C98S/E210C) were generated from a mouse cDNA clone subcloned into a pET-3d vector as previously described (*9, 10*). All plasmids were transformed into BL21(DE3) cells (Invitrogen) and expressed under isopropyl 1-thio-D-galactopyranoside induction. Cells were harvested and suspended in a CM buffer containing 30 mM citric acid, pH 6.0, 1 mM EDTA, 1 mM DTT, and protease inhibitors. After sonication and centrifugation, the supernatant was fractionated with ammonium sulfate. The pellets obtained from 30% to 60% of ammonium sulfate saturation were dissolved in a CM buffer and dialyzed against the buffer overnight. After centrifugation to remove any insoluble materials, the sample was loaded to a CM column. Proteins were eluted from the column with a gradient from 0 to 0.6 M NaCl. The purity of the proteins was checked with SDS gel. Cardiac Tm (cTm) (*11*), actin (*12*), and myosin subfragment 1(S1) from chymotryptic digestion of myosin (*13*) were obtained from bovine cardiac tissue.

Protein Labeling. Modification of the single-cysteine residues of cTnI mutants with IAEDANS was performed according to previously described procedures (*8, 10*). Briefly, the lyophilized protein was resuspended in a labeling buffer containing 50 mM Mops (pH 7.4), 3 M urea, 100 mM KCl, 1 mM EDTA, and 1 mM DTT and then stepwise dialyzed against the labeling buffer to reduce [DTT] to ~10 μM. Each single-cysteine cTnI (70−100 μM) was incubated with a 3 molar excess of IAEDANS under constant stirring overnight at 4 °C. Unreacted probes were reduced by adding DTT to a final concentration of 2 mM from a 1 M stock solution and then removed through dialysis. Modification of cysteine 374 of actin was carried out using a previously described procedure with modification (*14, 15*). The purified actin (2.5 mg/mL) was dialyzed against a buffer containing 50 mM Mops (pH 7.5), 100 mM KCl, 1 mM EDTA, and 1 mM DTT. DTT was reduced to 10 μM by dialyzing against the same buffer containing no DTT. The sample was mixed with a 5-fold molar excess of DABMI and incubated at 4 °C for 20 h. The reaction was terminated by adding 2 mM DTT. Unreacted probe was removed by centrifugation and dialysis. Label ratio was determined using $\varepsilon_{325nm} = 6000\ cm^{-1}\ M^{-1}$ for AEDANS and $\varepsilon_{460nm} = 24600\ cm^{-1}\ M^{-1}$ for DABM, respectively. The label ratios for all AEDANS-labeled cTnI mutants were >95%, and the ratio for actin was >93%. The identities of cTnI mutants and labeled proteins were verified using electrospray mass spectrometric analysis.

Reconstitution of Troponin Complex and Thin Filament. Reconstituted cardiac troponin was obtained using a previous procedure (*16*) with modifications. cTnC, cTnI, and cTnT were separately dialyzed against a reconstitution buffer (50 mM Tris-HCl, pH 8.0, 6 M urea, 500 mM KCl, 5 mM $CaCl_2$, 2 mM DTT) and then mixed at a 1.0:1.1:1.1 molar ratio (10, 11, and 11 μM final concentrations). The mixture was gently shaken for 2 hs at room temperature and then stepwise dialyzed against a high salt buffer containing 1 M KCl, 20 mM Mops (pH 7.0), 5.0 mM $MgCl_2$, 1.0 mM $CaCl_2$, and 1.5 mM DTT to successively reduce the urea concentration (6, 4, 2, and 0 M). The KCl concentration was subsequently reduced to 1, 0.7, 0.5, 0.3, and 0.15 M by stepwise dialysis against a working buffer containing 150 mM KCl, 50 mM Mops (pH 7.0), 5 mM $MgCl_2$, 2 mM EGTA, and 1 mM DTT. The sample was centrifuged to remove insoluble unbound cTnI and cTnT. The formation of the troponin complex and its stoichiometry were verified by native gel and SDS−PAGE electrophoresis. cTn−cTm complexes were formed by mixing cTn and cTm at a ratio of 1:1.1 (4 μM

cTn) in the same working buffer plus a sufficient volume of 3 M KCl to bring the final KCl concentration to 300 mM. Excessive salt was then reduced to 150 mM KCl in two dialysis steps. cTn−cTmA$_7$ was prepared by mixing cTn−cTm and polymerized actin at a ratio of 1:7.5 (2:15 μM) in the working buffer with 300 mM KCl, followed by reducing [KCl] to 150 mM as for the cTn−cTm complex. cTn−cTmA$_7$−S1−ADP was prepared by adding S1 to the cTn−cTmA$_7$ mixture at a ratio of 1:7:7 (cTn−cTm:actin:S1) after KCl had been decreased to 150 mM. Immediately prior to measurements, ADP was added to a final concentration of 4 mM from a MgADP stock solution prepared from $MgCl_2$ (200 mM) and Na_2ADP (200 mM) in the working buffer.

PKA Phosphorylation of cTnI. cTnI was phosphorylated by the catalytic subunit of PKA, using a cTnC affinity column (*17*). Briefly, a sample of purified cTnI mutant was loaded on a cTnC affinity column equilibrated in 50 mM KH_2PO_4 at pH 7.0, 500 mM KCl, 10 mM $MgCl_2$, and 0.5 mM DTT, followed by adding 125 units of PKA/mg of cTnI. To initiate the reaction, ATP was added to the column to a final concentration of 1.0 mM. After 30 min at 30 °C, the column was washed with a buffer containing 50 mM Mops at pH 7.0, 500 mM KCl, 2 mM $CaCl_2$, and 0.5 mM DTT. Phosphorylated cTnI was eluted with a buffer containing 6 M urea, 10 mM EDTA, 0.5 mM DTT, and 50 mM Mops at pH 7.0. The extent of phosphorylation was quantified by mass spectrometry and by treatment of the sample with alkaline phosphatase, followed by determination of inorganic phosphate using the EnzChek phosphate assay kit (*18*). Phosphorylation of the two PKA sites was >90%.

Acto-S1 ATPase Measurements. The biochemical activity of the labeled cTnI mutants was tested by Ca^{2+}-dependent regulation of acto-S1 ATPase activity. Measurements were performed at 30 °C in 60 mM KCl, 5.6 mM $MgCl_2$, 2 mM ATP, 30 mM imidazole (pH 7.0), 1 mM DTT, and either 500 μM $CaCl_2$ for the $+Ca^{2+}$ state or 1 mM EGTA for the $-Ca^{2+}$ state. The protein concentrations used were 4.2 μM F-actin, 0.6 μM cTm, 0.6 μM cTn, and 0.5 μM S1. The amounts of inorganic phosphate released were determined colorimetrically as previously reported (*19*). Absorption was measured at 630 nm with a Beckman DU-640 spectrophotometer.

Fluorescence Measurements. Steady-state fluorescence measurements of AEDANS were carried out on an ISS PCI photon-counting spectrofluorometer, using a band-pass of 3 nm on both the excitation and the emission monochromators. Time-resolved fluorescence and anisotropy decays were collected in the time domain using an IBH 5000U fluorescence lifetime system equipped with a 343 nm LED as the light source. Anisotropy decays of AEDANS attached to the selected residues of cTnI were determined by measuring the emission at 480 nm polarized in the vertical and horizontal directions with vertically polarized excitation. The polarized decay data were fitted to a biexponential function to recover the limiting anisotropy at zero time (*20*).

Total fluorescence intensity decays of AEDANS from the donor-alone and donor−acceptor samples were collected at 480 nm with a time-correlated single photon counting system associated with the IBH 5000U under identical experimental condition using a polarizer set to the magic angle. These decays were used to calculate the distribution of intersite distances between donor and acceptor as in previous work (*16, 21*) using the equation:

$$I_{DA}(r,t) = \sum_i \alpha_{Di} \exp[-(t/\tau_{Di}) - (t/\tau_{Di})(R_0/r)^6] \quad (1)$$

where $I_{DA}(r,t)$ is the distance-dependent donor intensity decay of a donor−acceptor pair separated by a given distance r, α_{Di} is the fractional amplitude associated with the lifetime τ_{Di} for the ith component, and R_0 is the Förster critical distance at which the energy transfer efficiency is 0.5 and can be experimentally derived for each specific FRET donor−acceptor pair. The experimentally determined R_0 for the AEDANS−DABM donor−acceptor pair was in the range of 40−43 Å for different protein preparations and biochemical states. These values were used to calculate distance distributions.

The observed donor intensity decay may be treated in the most general case as an ensemble of donor−acceptor pairs and is given by the average of the individual decays weighted by the distance probability distribution [$P(r)$] of the donor−acceptor pair (*22*):

$$I_{DA}(t) = \int_0^\infty P(r) I_{DA}(r,t)\, dr \quad (2)$$

The probability distribution is usually assumed to be a Gaussian with a mean distance (r) and a half-width (hw) of the distribution. The standard deviation (σ) of the Gaussian is related to the half-width by hw = 2.354σ. The distributions of the distances between the selected residues of cTnI and Cys374 of actin were calculated using Global Curve (*23*), a general purpose global nonlinear least-squares program. Confidence estimates from time-resolved FRET data were obtained using a grid search of the reduced chi square ratio (χ_R^2) as described (*23, 24*). An analysis of the dependence of this ratio on the mean distance and the half-width were used to judge goodness of fit for the distribution and determine the upper and lower estimates of the mean distance and the half-width at the 68% confidence level (*22, 25*).

RESULTS

Characterization of cTnI Mutants. To examine whether labeled cTnI mutants have the same regulatory function as wild-type protein, Ca^{2+} regulation of the actin-activated S1-ATPase activity was determined. The results are summarized in Table 1. The ATPase activity of acto-S1 in the absence of the regulatory proteins troponin and Tm was taken as 100%. The Ca^{2+} sensitivity was 0.785 for the control preparation containing wild-type cTn and Tm. The Ca^{2+} sensitivities for all other preparations containing labeled mutants of cTnI were similar to that of the control, suggesting that the effects of the mutations and modifications of cTnI on the Ca^{2+} regulatory activity were negligible.

SDS−PAGE and native gels were used to examine the stability and stoichiometry of the troponin complex reconstituted with mutant proteins and labeled cTnI. The complexes were reconstituted by incubating labeled cTnI mutants, cTnC, and cTnT in a molar ratio of 1.0:1.1:1.1 on ice for 30 min, and the reconstituted samples were then dialyzed against the working buffer containing 50 mM Mops (pH 7.0), 1 mM DTT, and 0.1 M KCl in the presence of 5 mM Mg^{2+}. The samples were centrifuged at 10000g for 10 min to remove insoluble cTnI and cTnT before gel electrophoresis. Figure

Table 1: Effects of Modified cTnI Mutants on Reconstituted Actomyosin ATPase Activity[a]

troponin complex	ATPase activity		Ca^{2+} sensitivity
	EGTA	Ca^{2+}	
cTnC(wt)−cTnT(wt)−cTnI(wt)	0.017	0.079	0.785
cTnC(wt)−cTnT(wt)−cTnI(Q131C)	0.015	0.074	0.797
cTnC(wt)−cTnT(wt)−cTnI(S151C)	0.019	0.084	0.773
cTnC(wt)−cTnT(wt)−cTnI(L160C)	0.016	0.079	0.797
cTnC(wt)−cTnT(wt)−cTnI(S167C)	0.018	0.085	0.788
cTnC(wt)−cTnT(wt)−cTnI(S188C)	0.017	0.077	0.779
cTnC(wt)−cTnT(wt)−cTnI(S210C)	0.016	0.072	0.778

[a] Ca^{2+}-dependent acto-S1 ATPase activity was measured at 30 °C in 60 mM KCl, 5.6 mM $MgCl_2$, 2 mM AP, 30 mM imidazole (pH 7.0), 1 mM DTT, and either 500 μM $CaCl_2$ for the Ca^{2+} state or 1 mM EGTA for the EGTA state. The protein concentrations used were 4.2 μM F-actin, 0.6 μM cTm, 0.6 μM cTn, and 0.5 μM S1. The amounts of inorganic phosphate released were determined colorimetrically and expressed in μmol of P_i s^{-1} g^{-1} (*19*). Ca^{2+} sensitivity was defined as 1 − ($activity_{EGTA}$/$activity_{Ca}$) (*19*). cTnC(wt), cTnI(wt), and cTnT(wt) are wild-type cTnC, cTnI, and cTnT, respectively. The cTnI mutants were labeled at the single cysteine with AEDANS.

1 shows that both wild-type and mutant troponin complexes existed as single complexes with the correct stoichiometry (Figure 1). Multiple experiments were performed on samples prepared within 3 weeks, and gels showed no evidence of protein degradation.

Conformational Changes in cTnI at the Actin−cTnI Interface. Fluorescence of the donor AEDANS attached to the six single-Cys residues in the C-terminal region of cTnI in reconstituted thin filaments was quenched in the presence of the acceptor DABM attached to C374. The extent of quenching was dependent upon donor location in cTnI (data not shown). Differences in donor quenching reflected differences in energy transfer and suggested different intersite distances between actin C374 and the cTnI sites. The quenching was also sensitive to the presence of Ca^{2+}, indicating a Ca^{2+}-induced alteration of the intersite distances. Figure 2 shows a series of donor intensity decay plots with the donor attached to cTnI residue 167 and the acceptor attached to actin C374 in different ionic environments and biochemical states. These decays were analyzed in terms of a distribution of the distances between donor and acceptor (eq 2). Figure 3 shows a typical analysis of one of the tracings from Figure 2 for the intensity decay of the donor attached to cTnI(167C). The distributions of this intersite distance determined in four biochemical states are shown in Figure 4. Summarized in Table 2 are distance results for the six distances between actin(C374) and the cTnI sites. In the absence of Ca^{2+} (Mg^{2+} alone), the mean distance between actin and cTnI(167C) was 40.8 Å and the half-width of the distribution was 19.0 Å. In the presence of Ca^{2+} (Mg^{2+} + Ca^{2+}), the distance increased by 12.3 Å to 53.1 Å and the half-width decreased by 3.8 Å to 15.2 Å. This effect of Ca^{2+} on the distance is similar to that previously reported for an equivalent intersite distance in skeletal thin filament (*15*). Similarly, bound Ca^{2+} also induced an increase in the actin−cTnI(C160) distance by 10.2 Å from 47.1 to 57.3 Å and a decrease in the half-width of the distance distribution by 4.9 Å from 19.5 to 14.6 Å. Myosin S1 strongly bound to thin filaments lengthened these two distances regardless of whether Ca^{2+} was absent (Mg^{2+} alone) or present (Mg^{2+} + Ca^{2+}) and in each ionic condition. Bound S1 increased the half-widths of the distributions (0.6−4.2 Å). However, bound Ca^{2+} reduced the half-width of the distributions of both distances determined with thin filaments containing bound S1. Taken together, these results suggested that Ca^{2+} binding to cTnC in thin filaments induced a separation between the regulatory region of cTnI and the C-terminus of actin. This separation was further increased by the strong binding of myosin. The decrease in the half-width of the distance distributions induced by Ca^{2+} binding with or without bound S1 suggested a loss of conformational flexibility in the region between the actin C-terminus and the regulatory region of cTnI.

Within the inhibitory region of cTnI, Ca^{2+} binding induced a small increase (>2 Å) in the distance between actin and cTnI(131C) and a larger increase (11.1 Å) in the other distance between actin and cTnI(151C). The half-widths of these two distance distributions also increased from the Mg^{2+} state to the Ca^{2+} state. Similar Ca^{2+}-induced increases were also observed in the presence of strongly bound S1. cTnI residue 131 is located at the N-terminal end of the inhibitory region and adjacent to the cTnI−cTnC interface, and residue 151 is located at the junction between the inhibitory and regulatory regions. These two regions are contiguous and expected to move together by Ca^{2+} and S1 binding. The inhibitory region of cTnI is expected to be released from actin by Ca^{2+} binding, and this release conferred a more flexible inhibitory region as reflected by increases in the half-widths of the distance distributions.

In the second actin-binding region or the mobile domain of cTnI (residues 188 and 210), small increases in intersite distances (4.6−5.8 Å) between actin and these two residues were induced by Ca^{2+}. The half-widths of the distance distributions were more than a factor of 2 smaller than those for the other distributions regardless of whether Ca^{2+} was absent or present (5.4−8.6 Å). These narrower distributions suggested that the second actin-binding region in cTnI is relatively rigid in comparison with the other regions of cTnI in the thin filament. This finding is in general agreement with the reported rigid helical structure of the second binding region of cTnI in the core domain of cTn (*26*), the organized structure of this actin-binding domain in the absence of Ca^{2+} demonstrated by NMR (*27*), and results from EM reconstruction (*28*). Strongly bound S1 lengthened these two intersite distances, but its effect on the half-widths of the two distance distributions was small (<1 Å).

The thin filament is organized around a central filament of actin, which can be viewed as a single left-handed genetic helix of actin monomers. Each regulatory unit of the thin filament is comprised of 1 cTn, 1 cTm, and 7 actin monomers. This structure potentially can give rise to FRET from a donor attached to a cTnI residue to an acceptor attached to a given residue in both the nearest actin monomer ($actin_0$) and the next nearest monomer ($actin_{-1}$). If such multiple transfer occurred, the observed transfer efficiency would contain a contribution of transfer to $actin_{-1}$. The calculated intersite distance would be an underestimate. In a previous modeling study (*29*), we showed that the contribution of transfer to $actin_{-1}$ from skeletal TnI residue 133 (equivalent to residue 167 in cTnI) to actin 374 was negligible. This result suggests that, in the present cardiac thin filament system, transfer from cTnI(167) to actin 374 in $actin_{-1}$ would be negligible. To further examine this problem, using the software Chimera, we fitted cardiac

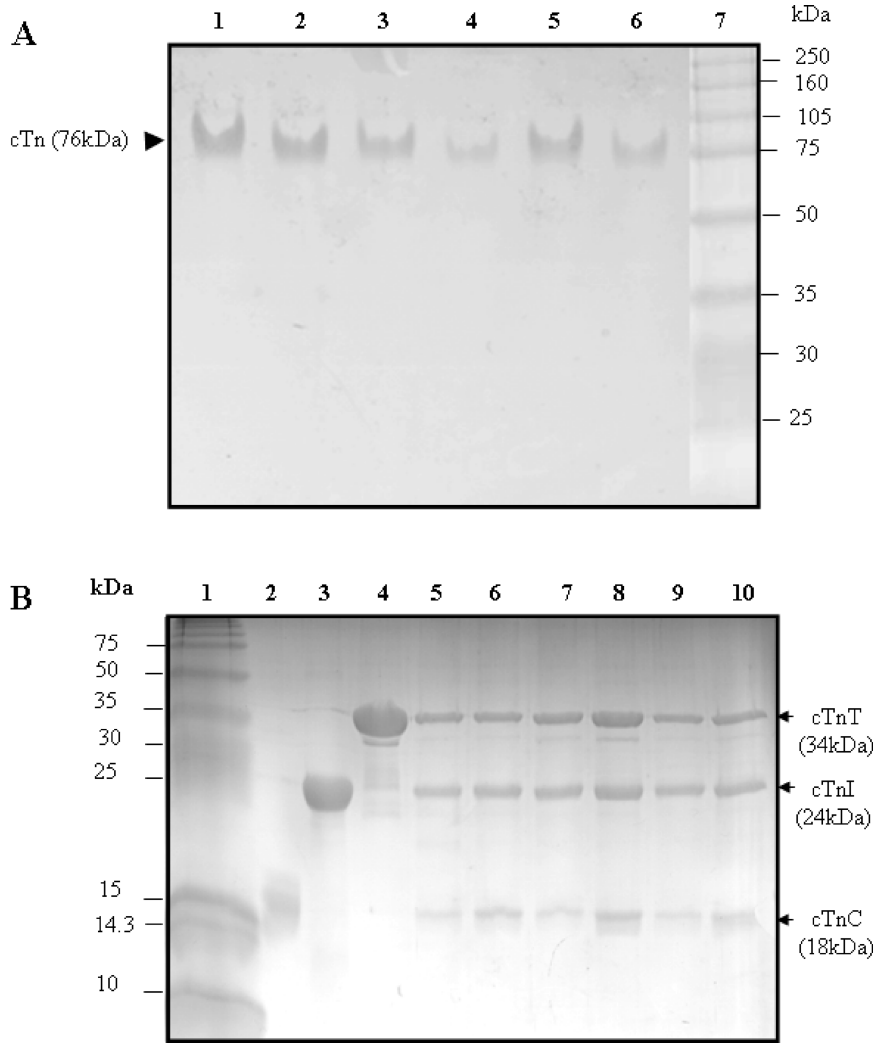

FIGURE 1: Electrophoresis analysis of reconstituted cardiac troponin. Panel A: Native PAGE gels (8% resolving and 4% stacking). Lanes 1−6: Troponin reconstituted from wild-type cTnC, wild-type cTnT, and a cTnI mutant in which the single cysteine was labeled with AEDANS. Lane 7: HMW protein standards (Amersham Biosciences). (1) cTnI(131C), (2) cTnI(151C), (3) cTnI(160C), (4) cTnI(167C), (5) cTnI(188C), and (6) cTnI(210C). These gels showed all six reconstituted samples ran as a single component with a mass of ~76 kDa. Panel B: SDS−PAGE gels (18% resolving and 4% stacking). Lane 1: LMW protein standards (Amersham Bisciences). (2) Wild-type cTnC, (3) wild-type cTnI, and (4) wild-type cTnT. Lanes 5−10: Troponin reconstituted from wild-type cTnC, wild-type cTnT, and a cTnI mutant in which its single cysteine was labeled with AEDANS. (5) cTnI(131C), (6) cTnI(151C), (7) cTnI(160C), (8) cTnI(167C), (9) cTnI(188C), and (10) cTnI(210C). The six reconstituted troponin samples were each resolved into three bands. Densitometry analysis of the bands was done with Bio-Rad Quantity One software, and the results showed that the three resolved bands corresponded to cTnC, cTnI, and cTnT with a molar ratio of 1:1:1. No significant degradation products were found on the gels.

troponin onto the published EM maps of cardiac thin filaments (*30*) and estimated the distances between actin 374 in actin$_{-1}$ and the cysteine residues of cTnI(160), cTnI(167), cTnI(188), and cTnI(210). These distances were $>1.7R_0$, which are too large and would contribute negligibly to the observed transfer efficiency. The estimated distances from the other two sites, cTnI(130) and cTnI(151), to actin$_{-1}$ were shorter, with potential secondary contributions to the observed transfer efficiency of 16−17%. Since these shorter distances were close to the value of R_0 and because of the inverse sixth power relationship between transfer efficiency and intersite distance, the error in the two calculated distances would be <5%.

We used a value of $^2/_3$ for the orientation factor κ^2 assuming that both donor and acceptor tumbled rapidly and isotropically. If ligand binding to the thin filament substantially modified probe mobility, a different value would be needed to calculate distance parameters for systems containing bound Ca^{2+} and S1. However, the acceptor was non-fluorescent, and it was not feasible to evaluate the possible range of κ^2 for our calculation. We measured the anisotropy decay of the donor probe attached to each of the six sites in cTnI and determined the anisotropies associated with the attached probe. All anisotropy decays are resolved into two components. The short component is a few nanoseconds for all decays and accounts for ~40% of the recovered total anisotropy (data not shown). The calculated anisotropies showed very similar donor mobility in all systems, suggesting that ligand binding to the thin filaments did not appreciably affect the mobility of the donor in the cTnI sites. The observed changes in both intersite distance and the half-width of the distance distribution induced by bound Ca^{2+} and S1 reflected a conformational effect and not a change in donor mobility.

To further investigate the effect of strongly bound S1 on the six intersite distances, we used a second preparation of thin filaments reconstituted with a cTnC mutant (D65V/D67A) to repeat distance measurements. This mutant cannot

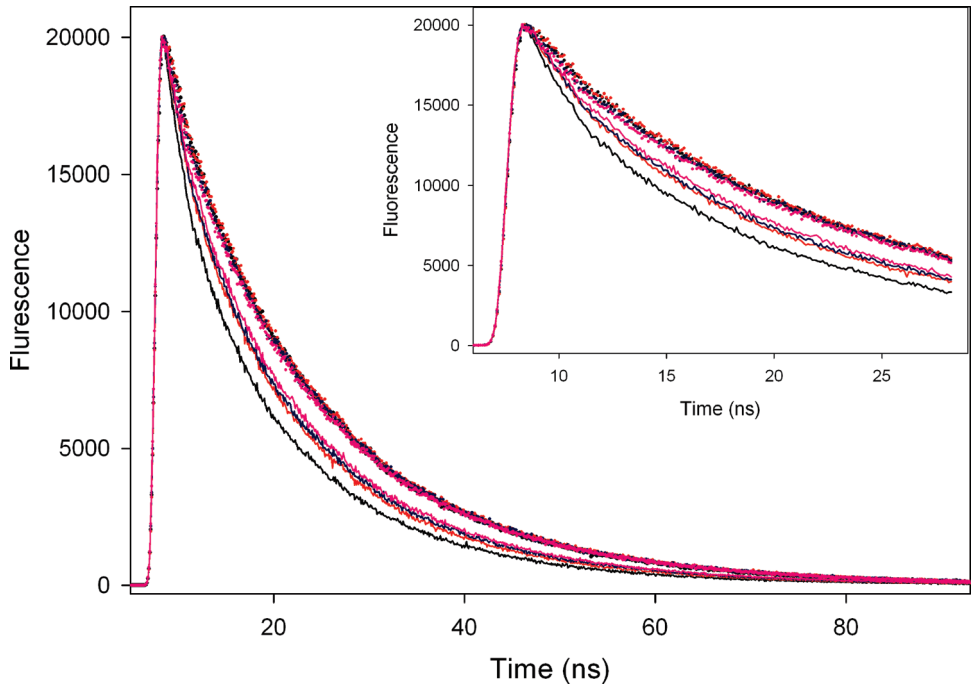

FIGURE 2: Fluorescence intensity decays of AEDANS (donor) attached to residue 167 of cTnI in reconstituted cardiac thin filaments. Dotted curves, donor-only sample; solid curve, donor−acceptor sample in which actin was labeled with acceptor DABM at C374. Black, no Ca^{2+} (Mg^{2+} only); red, Ca^{2+} (+Mg^{2+}); pink, myosin S1 is strongly bound to the filaments and in the absence of Ca^{2+}; blue, myosin is strongly bound to the filaments and in the presence of Ca^{2+}. The decays were measured with excitation at 343 nm, and the emission was collected at 500 nm using a channel width of 100 ps. Samples were in 50 mM Mops at pH 7.0, 1 mM DTT, 1 mM EGTA, 5 mM $MgCl_2$, and 0.2 M KCl. When Ca^{2+} was present, it was 2 mM $CaCl_2$. The initial fast decays of these tracings are shown in the inset.

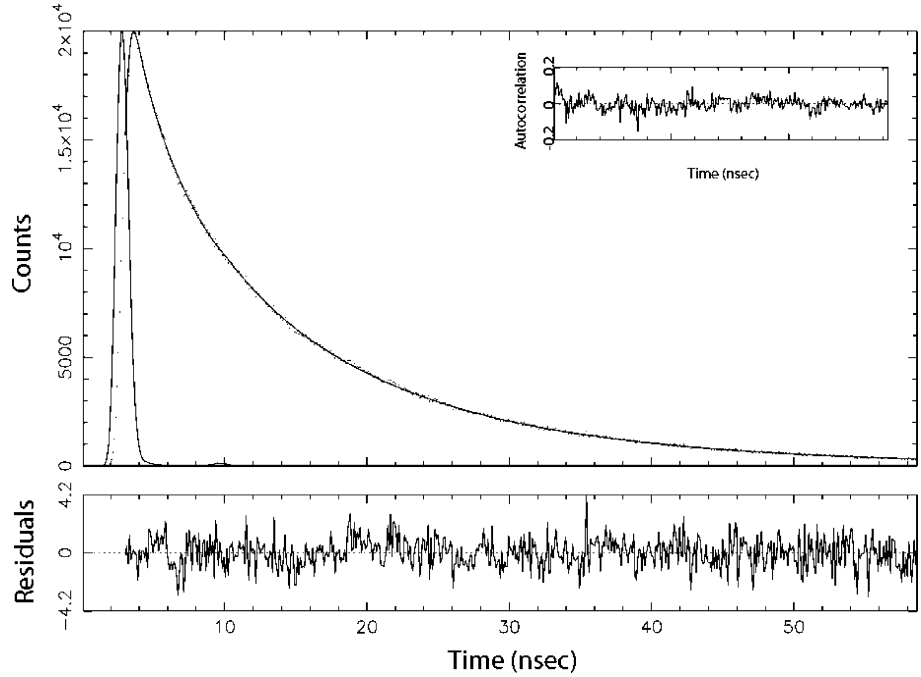

FIGURE 3: An analysis of energy transfer from AEDANS attached to cTnI(167C) to DABM attached to actin(C374) in reconstituted cardiac thin filaments. The analysis shown here is for the corresponding decay curve shown in Figure 2. The sharp peak on the left is the excitation light pulse. The donor intensity decay in the presence of acceptor (broad peak on the right) was fit to eq 2 with a single Gaussian as $P(r)$ and a sum of two exponential terms for $I_{DA}(r,t)$ (eq 1). The residual plot of the fit is displayed in the lower panel across the figure, and the autocorrelation plot is shown as an inset at the upper right-hand corner. The best-fit data from this analysis were used to calculate the distribution of the intersite distances between cTnI C167 and actin C374.

chelate Ca^{2+} because the first and third acidic residues within the 12-residue Ca^{2+}-binding loop were replaced by hydrophobic side chains (*31*). The results are summarized in Table 3. As expected, Ca^{2+} had no effect on all six intersite distances and negligible effects (within experimental errors) on the half-widths of the distributions. Bound S1 conferred increases in the distances in the range of 4−10 Å. This range was comparable to the changes observed (4−14 Å) with the preparation that were reconstituted with functionally competent cTnC (Table 2). With the exception of the actin−cTnI(210C) distance, bound S1 induced small increases in the half-width (2.8−4.7 Å) of the other five distributions. These increases

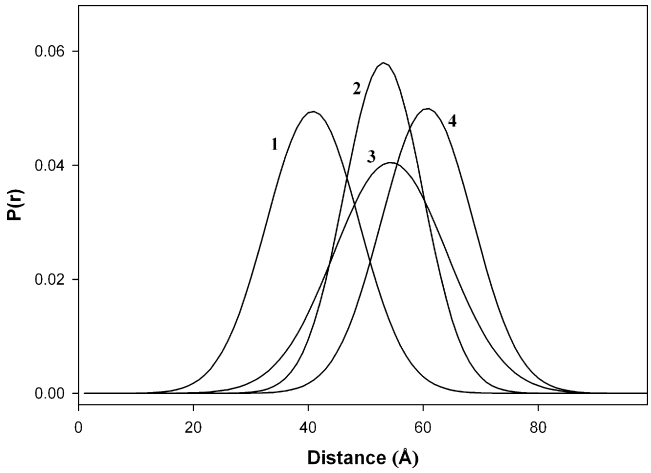

FIGURE 4: Area-normalized distributions of intersite distances between actin C374 and cTnI(167C) in cardiac thin filaments in different biochemical states: (1) in the absence of Ca^{2+}, (2) in the presence of Ca^{2+}, (3) in the presence of strongly bound myosin S1 ($-Ca^{2+}$), and (4) in the presence of strongly bound S1 ($+Ca^{2+}$).

were similar to those (0.2−2.5 Å) elicited by bound S1 in Ca^{2+}-competent thin filaments. The distribution of the distance actin−cTnI(210C) showed a decrease (−4.6 Å) in the half-width with thin filaments complexed with S1. A marginal decrease (−0.5 Å) in the half-width of the distribution of the same actin−cTnI(160C) distance was also observed with thin filaments containing functionally competent cTnC. Taken together, these results showed that bound S1 alone was capable of inducing a separation of the C374 region of actin from several regions of cTnI.

The results listed in Tables 2 and 3 were obtained with thin filament preparations to which cations were first added, followed by addition of S1 + ADP. Each addition resulted in an increase in the distance. It was of interest to establish whether the increase elicited by bound S1 was independent of the cation state. Additional experiments were performed in which S1 was first added, followed by the addition of Ca^{2+}. The two sets of results for the distance between actin and cTnI(C167) are summarized in Figure 5 in a closed pathway. Starting from the initial state of the thin filament in the presence of Mg^{2+} ($TF\cdot Mg^{2+}$), the clockwise pathway showed an increase of 9 Å in the distance induced by bound Ca^{2+} in the intermediate state and an additional increase of 10.6 Å by the subsequent addition of S1−ADP to form the final state, $TF\cdot S1\cdot Mg^{2+}\cdot Ca^{2+}$. The counterclockwise pathway showed an increase of 13.5 Å in the initial step in which S1−ADP was added and a second increase of 6.4 Å induced by the addition of Ca^{2+} to reach the same final state. The sum of the two increases was the same for the two pathways. This additive effect was also observed in the other five actin−cTnI distances, with differences between the two pathways in each case being $<\pm 0.2$ Å. The experiments with thin filaments reconstituted from a nonfunctional cTnC mutant (Table 3) were repeated by reversing the order of addition of Ca^{2+} and S1−ADP. The total distance increases from actin to each cTnI site between the initial and final states were within 0.1−0.3 Å of both the clockwise pathway and counterclockwise pathway (results not shown). These results suggested that the conformational effect of strongly bound S1 on the disposition of the C-terminus of actin from functionally important regions of cTnI was not influenced by the presence of functional cTnC.

The unique N-terminal extension of cTnI has two PKA sites (Ser23 and Ser24). In a previous study we reported that bisphosphorylation of these two sites resulted in a bending of this segment toward the C-terminus (*32*). We investigated the effects of bisphosphorylation of cTnI on the proximity relationship between actin Cys374 and four of the six sites in cTnI (residues 131, 151, 160, and 167) in regulated thin filaments. These results are summarized in Table 4. Bisphosphorylation increased the distance from actin to cTnI(131) by 7 Å in the presence of Mg^{2+} and an increase of 5 Å in the presence of both Mg^{2+} and Ca^{2+}. The difference of 1.7 Å was observed with nonphosphorylated thin filaments between the two ionic environments. This distance in the bisphosphorylated preparation was not sensitive to Ca^{2+} (Table 4). Bound S1 induced a small change in the distance (2.1 Å) in the presence of Mg^{2+} and a larger increase in the distance (5.2 Å) in the presence of both Mg^{2+} and Ca^{2+} between the two sites in which cTnI was bisphosphorylated. The effects of bisphosphorylation on the changes of the distances from actin to the other three cTnI sites were negligibly smaller (±1 Å), except that a change of 2.2 Å between actin and cTnI(151) was observed in the presence of Ca^{2+} and strongly bound S1. The distributions of the four distances determined with bisphosphorylated cTnI were all narrower than the corresponding distributions from thin filaments containing nonphosphorylated cTnI. The half-widths of these narrower distributions were smaller than those from the corresponding nonphosphorylated samples by 1−10 Å. These results may suggest that phosphorylation of the N-terminus of cTnI can affect the structural dynamics of the regulatory and inhibitory regions of cTnI at the interface between cTnI and actin.

DISCUSSION

Regulation of cardiac thin filaments is triggered by Ca^{2+} binding to cTnC which results in a series of conformational changes within the filament, including changes in the actin−cTnI interaction. In the present study, we have determined FRET between a donor attached to several residues in the C-terminal region of cTnI and an acceptor attached to actin C374 in its C-terminus. Results from these measurements enable us to investigate conformational changes that occur at the interface between actin and the C-terminal region of cTnI resulting from the binding of regulatory Ca^{2+} and myosin and bisphosphorylation of cTnI in its N-terminal extension.

The FRET results on increases in intersite distance from the penultimate residue of actin to several sites in the C-terminal region of cTnI suggest large Ca^{2+}-induced movements (10−12 Å) of the regulatory region of cTnI away from actin C-terminus. These large Ca^{2+}-induced increases in the distances are accompanied by smaller changes in distances from the actin C-terminus to the N-terminus of the inhibitory region (<3 Å, residue 131) and to the second actin-binding region (<6 Å, residues 188 and 210) of cTnI. A recent structural study of skeletal thin filament using X-ray fiber diffraction suggests that Ca^{2+} binding has little effect on troponin core domain orientation on actin, but the gravity center of the thin filament is slewed and troponin C moves 2 Å outward from the actin surface (*33*). The slewed shifting of the thin filament center observed in this study is likely

Table 2: FRET Distances between Actin(C374) and cTnI in Regulated Cardiac Thin Filaments[a]

		thin filament		thin filament + S1-ADP	
distance	conditions	mean distance (Å)	half-width (Å)	mean distance (Å)	half-width (Å)
cTnI(131C)−actin(C374)	Mg^{2+}	37.3 (36.3, 38.5)	12.8 (11.2, 13,7)	41.4 (40.0, 42.9)	15.0 (13.9, 16.3)
	$Mg^{2+} + Ca^{2+}$	39.0 (38.1, 40.3)	15.1 (14.3, 16.4)	44.0 (42.8, 45.1)	21.5 (20.3, 22.9)
cTnI(151C)−actin(C374)	Mg^{2+}	43.5 (42.8, 44.2)	13.0 (12.1, 13.7)	53.9 (52.6, 55.1)	18.0 (16.9, 19.6)
	$Mg^{2+} + Ca^{2+}$	54.6 (53.2, 55.8)	17.1 (16.3, 17.8)	56.8 (55.6, 57.8)	22.7 (20.9, 23.3)
cTnI(160C)−actin(C374)	Mg^{2+}	47.1 (45.9, 48.0)	19.5 (18.2, 20.8)	56.3 (54.0, 58.1)	21.6 (20.2, 22.8)
	$Mg^{2+} + Ca^{2+}$	57.3 (56.3, 58.6)	14.6 (12.4, 16.3)	59.8 (58.3, 61.7)	15.2 (13.6, 17.1)
cTnI(167C)−actin(C374)	Mg^{2+}	40.8 (39.3, 41.7)	19.0 (18.1, 20.3)	54.3 (53.8, 55.9)	23.2 (21.9, 24.1)
	$Mg^{2+} + Ca^{2+}$	53.1 (52.2, 54.3)	15.2 (14.3, 16.6)	60.7 (59.2, 62.2)	17.3 (15.9, 18.4)
cTnI(188C)−actin(C374)	Mg^{2+}	46.7 (45.8, 47.7)	6.6 (6.1, 7.3)	53.7 (52.1, 55.3)	6.8 (6.2, 7.3)
	$Mg^{2+} + Ca^{2+}$	51.3 (50.2, 52.5)	8.6 (7.8, 10.2)	58.4 (57.2, 59.6)	9.6 (8.7, 11.2)
cTnI(210C)−actin(C374)	Mg^{2+}	47.3 (46.1, 48.4)	5.4 (4.9, 5.8)	54.2 (53.2, 55.2)	4.9 (4.3, 5.6)
	$Mg^{2+} + Ca^{2+}$	53.1 (52.0, 54.3)	7.2 (6.4, 8.3)	57.5 (56.4, 59.0)	8.4 (6.9, 9.8)

[a] Numbers in parentheses are the lower and upper bounds of the best-fitted parameters at the 68% confidence level (one standard deviation). Thin filament + S1-ADP was prepared by mixing each troponin component at a ratio of 1 cTn, 1 cTm, 7.5 polymerized actin, and 7 S1-ADP (see Materials and Methods).

Table 3: FRET Distances from Actin C374 to cTnI in Cardiac Thin Filaments Reconstituted with cTnC Mutant D65V/D67A Which Does Not Bind Regulatory Ca^{2+}[a]

		thin filament		thin filament + S1-ADP	
distance	conditions	mean distance (Å)	half-width (Å)	mean distance (Å)	half-width (Å)
cTnI(131C)−actin(C374)	Mg^{2+}	38.3 (37.1, 40.0)	15.8 (14.2, 16.7)	42.6 (41.3, 43.9)	20.5 (19.3, 21.9)
	$Mg^{2+} + Ca^{2+}$	37.7 (36.5, 38.9)	15.7 (14.3, 16.8)	44.9 (43.8, 46.1)	19.0 (17.9, 19.9)
cTnI(151C)−actin(C374)	Mg^{2+}	46.4 (45.8, 47.2)	10.5 (9.1, 11.7)	51.7 (50.9, 52.8)	15.3 (13.4, 16.0)
	$Mg^{2+} + Ca^{2+}$	46.2 (45.0, 47.1)	14.2 (13.4, 15.1)	52.1 (51.5, 52.9)	18.4 (16.7, 19.9)
cTnI(160C)−actin(C374)	Mg^{2+}	47.3 (46.5, 48.3)	16.3 (15.8, 16.7)	54.6 (53.7, 55.9)	20.6 (19.7, 21.6)
	$Mg^{2+} + Ca^{2+}$	47.9 (46.8, 48.6)	17.2 (16.8, 17.7)	56.6 (55.3, 57.5)	20.7 (19.6, 21.5)
cTnI(167C)−actin(C374)	Mg^{2+}	43.1 (42.0, 43.9)	19.4 (18.9, 19.8)	52.4 (51.7, 53.7)	22.7 (21.9, 23.5)
	$Mg^{2+} + Ca^{2+}$	42.4 (41.8, 43.7)	21.1 (20.7, 21.9)	53.5 (52.2, 54.7)	23.4 (21.7, 26.0)
cTnI(188C)−actin(C374)	Mg^{2+}	46.1 (45.3, 47.5)	4.3 (3.9, 4.6)	56.1 (55.2, 57.8)	7.1 (6.6, 7.7)
	$Mg^{2+} + Ca^{2+}$	46.8 (45.3, 47.9)	6.0 (5.7, 6.6)	56.0 (55.1, 57.4)	10.8 (9.9, 11.1)
cTnI(210C)−actin(C374)	Mg^{2+}	48.8 (47.8, 49.6)	11.6 (10.8, 12.4)	54.3 (53.2, 55.7)	7.0 (6.6, 7.4)
	$Mg^{2+} + Ca^{2+}$	49.0 (48.1, 50.4)	10.7 (9.9, 11.3)	54.6 (53.7, 55.7)	3.6 (3.3, 3.8)

[a] Numbers in parentheses are the lower and upper bounds of the best-fitted parameters at the 68% confidence level (one standard deviation).

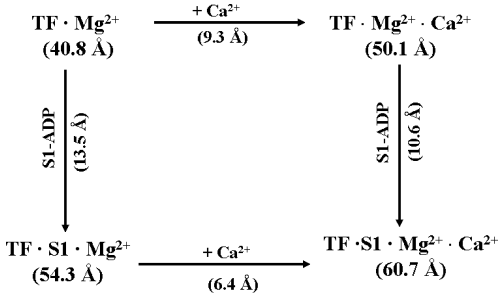

FIGURE 5: A cyclic representation of the FRET distance between actin C374 and cTnI C167C in cardiac thin filaments (TF) determined in three states. The initial complex is TF•Mg^{2+} in the Mg^{2+} state in which the distance is 40.8 Å. In the clockwise direction, Ca^{2+} binding to TF•Mg^{2+} to form the second complex TF•Mg^{2+}•Ca^{2+} increases the distance by 9.3 Å, and the subsequent binding of S1 to form the final complex TF•S1•Mg^{2+}•Ca^{2+} (right vertical pathway) lengthens the distance by an additional 10.6 Å. The sum of the two increases in these two clockwise steps is 9.3 + 10.6 = 19.9 Å. In the counterclockwise pathway, S1 first binds to TF•Mg^{2+} to form TF•S1•Mg^{2+}, increasing the distance by 13.5 Å. Ca^{2+} binding to form the final complex TF•S1•Mg^{2+}•Ca^{2+} (lower pathway) lengthens the distance by another 6.4 Å. The sum of these two increases in the counterclockwise direction is 13.5 + 6.4 = 19.9 Å. The difference in the distances between TF•Mg^{2+} (initial state) and TF•S1•Mg^{2+}•Ca^{2+} (final state) is 19.9 Å (60.7 − 40.8), independent of how the final state is reached, whether along the clockwise or the counterclockwise direction.

correlated to the movements of the C-domain of cTnI detected by our FRET measurements. These movements are a consequence of the movement of the regulatory region away from actin toward the Ca^{2+}-bound N-domain of cTnC in which a hydrophobic segment of the N-domain interacts with hydrophobic residues of the regulatory region. This sliding of the regulatory region drags along the contiguous inhibitory region, thus converting its helix−loop−helix motif into an extended segment (*10, 34*) and releasing the inhibitory region from actin. Such a "drag and release" mechanism (*16, 35, 36*) is consistent with the observed large increases of the distances from actin to the cTnI regulatory region and to the C-terminus of the inhibitory region and a smaller increase in the distance from actin to the N-terminus of the cTnI inhibitory region (residue 131, <3 Å). These Ca^{2+}-induced increases in the distances in the cTnI−actin interface would allow movements of tropomyosin on the actin surface to expose sites for interaction with cross-bridges. These distances between the actin C-terminus and cTnI sites are further increased by the binding of myosin S1 + ADP (2−7 Å). These additional increases are elicited by strong interactions between S1 and actin, equivalent to strong cross-bridge formations in muscle. These two-step changes in the distances between cTnI and actin revealed by our FRET are consistent with the three-state model for activation of thin filaments (*37, 38*). Recently, a FRET kinetic study of skeletal thin filament has reported that Ca^{2+} binding and subsequent strong cross-bridge interaction increased the distance between actin 374 and Cys133 of skeletal TnI (equivalent to Cys167 of cTnI) by 9 and 8 Å, respectively (*39*). These results are

Table 4: FRET Distances from Actin C374 to cTnI in Cardiac Thin Filaments Reconstituted with Bisphosphorylated cTnI[a]

		thin filament		thin filament + S1-ADP	
distance	conditions	mean distance (Å)	half-width (Å)	mean distance (Å)	half-width (Å)
p-cTnI(131C)−actin(C374)	Mg^{2+}	44.3 (43.1, 45.6)	11.5 (10.2, 13.6)	46.4 (44.3, 58.3)	12.4 (11.9, 15.9)
	Mg^{2+} + Ca^{2+}	44.3 (43.4, 45.4)	12.0 (10.8, 13.3)	49.5 (48.4, 50.3)	14.4 (12.7, 16.9)
p-cTnI(151C)−actin(C374)	Mg^{2+}	44.9 (43.6, 55.7)	9.5 (6.9, 11.6)	53.5 (52.1, 54.5)	11.7 (11.0,12.4)
	Mg^{2+} + Ca^{2+}	53.4 (52.0, 55.2)	7.0 (6.2, 7.7)	59.0 (48.0, 50.3)	10.1 (9.3, 11.1)
p-cTnI(160C)−actin(C374)	Mg^{2+}	48.3 (47.1, 49.6)	10.3 (9.4, 11.1)	56.2 (55.1, 57.7)	9.9 (8.3, 11.4)
	Mg^{2+} + Ca^{2+}	58.0 (56.8, 59.3)	11.1 (9.7, 12.8)	60.1 (58.9, 61.6)	12.8 (11.1, 14.3)
p-cTnI(167C)−actin(C374)	Mg^{2+}	42.1 (41.0, 43.4)	15.1 (14.2, 15.9)	55.4 (54.2, 56.8)	16.2 (15.6, 16.9)
	Mg^{2+} + Ca^{2+}	54.0 (52.7, 55.4)	12.7 (10.9, 14.3)	60.0 (59.0, 61.4)	11.7 (11.1, 12.7)

[a] Numbers in parentheses are the lower and upper bounds of the best-fitted parameters at the 68% confidence level (one standard deviation).

consistent with our results that the cTnI−actin interaction involves two steps.

Our FRET distance measurements have also shown that bound S1 alone can also lengthen the intersite distances in the absence of bound regulatory Ca^{2+} or in the presence of an inactivated Ca^{2+} binding site II in cTnC. If thin filament activation requires structural transitions resulting from separations of regions of cTnI from actin to allow movements of tropomyosin, the present results would suggest that either bound Ca^{2+} or bound myosin alone could elicit partial activation since the binding of each ligand independently results in increases in intersite distances. Full activation, however, would require both bound Ca^{2+} and strongly bound myosin allow complete movements of tropomyosin. An early study showed that activation of thin filaments by strongly bound myosin was independent of bound Ca^{2+} (*40*), but a recent study showed that both bound ligands are required for maximal activation of skeletal thin filaments (*41*).

The distribution of intersite distances provides a qualitative assessment of the dynamics of the interaction between the two sites and conformational flexibility between two regions within a molecular complex. The half-widths of the distributions of the two distances from actin to the residues (131 and 151) in the inhibitory region of cTnI are very similar and suggest a moderate conformational flexibility between the actin C-terminus and this region of cTnI in the absence of bound Ca^{2+}. Residue 131 is within the N-terminal helical segment of the inhibitory region that is followed by a segment (residues 134−145) predicted to be in a coil conformation (*42*). Residue 151 is located in the helical segment that follows the flexible coil. In the absence of bound Ca^{2+}, the flexible coil is thought to be bound to actin. The two flanking helical segments appear to have moderate conformational flexibility within the actin−cTnI complex. Bound Ca^{2+} releases the flexible segment of cTnI from actin, and this results only in small increases (2−4 Å) in the half-width of the distance distributions. Thus, dissociation of bound Ca^{2+} does not lead to a large gain in conformation flexibility between the two end segments of the cTnI inhibitory region.

Strongly bound S1 increases the half-width of the two distance distributions by 5−6 Å, thus conferring additional conformational flexibility. On the other hand, the half-widths of the distributions for the two distances from actin to the regulatory region (cTnI residues 160 and 167) are 6 Å larger than those for the inhibitory region in the absence of bound Ca^{2+}. This larger flexibility is reasonable since the regulatory region is some distance away from the loop segment of the inhibitory region. In the presence of bound Ca^{2+}, these larger half-widths are reduced by 4−5 Å. This loss of conformational flexibility occurs because the regulatory region has moved into the Ca^{2+}-induced open N-domain of cTnC in which much of the regulatory region is restricted due to a hydrophobic interaction between cTnC and the regulatory region.

The second actin-binding domain in the C-terminal segment of cTnI has no contact with cTnC or cTnT within the core structure of troponin. The distributions of the distances from the actin C-terminus to cTnI residues 188 and 210 are narrow with half-widths being 5−7 Å in the absence of Ca^{2+}. Bound Ca^{2+} and S1 confer only marginal broadening of the distributions, indicative of restricted conformational flexibility of the residues relative to the actin C-terminus. An α-helix is formed between cTnI residues 165 and 189 in the crystal structure (*26*), and the C-terminus (residues 170−211) is the putative second actin-binding site in the absence of Ca^{2+} (*43*). A recent NMR study shows that the mobile domain or the second actin-binding domain of skeletal TnI containing residues 131−182, corresponding to the residues 164−210 of cTnI, forms a helix (residues 132−140), a miniglobular subdomain (residues143−167), and a helix (residues 170−177) (*27*). The structural model constructed by docking of the NMR-derived mobile domain structure into the cryoelectron microscopy density map of the thin filament suggests an interaction between the domain of TnI and the outer domain of actin in the absence of Ca^{2+}. Similarly, a recent 3D electron microscopy reconstruction with the C-domain of cTnI containing residues 131−210 shows that, in the absence of Ca^{2+}, the C-domain of cTnI stretching across from $actin_{-0}$ (on which the troponin head would be located) to interact with subdomain 1 of $actin_{-1}$ (*28*). These observed structural features are consistent with the narrow distributions of the FRET distances reported in this study. A latching mechanism proposed for the regulatory role of cTnI in a recent study suggests that the second or "mobile" actin-binding domain of cTnI is highly dynamic in the presence of Ca^{2+} and becomes more structural upon interaction with actin in the absence of Ca^{2+} (*44*). However, the present results suggest that regions around two of these residues have limited flexibilities either in the presence or in the absence of bound Ca^{2+}.

Phosphorylation of the two serines at residues 23 and 24 of cTnI by PKA plays important roles in modulation myofilament Ca^{2+} sensitivity and cross-bridge kinetics (*6*). Evidence has suggested that in the absence of phosphorylation the N-terminal segment of cTnI interacts with the N-domain of cTnC and stabilizes the open conformation of the domain (*17, 45, 46*). Bisphosphorylation of cTnI induces

a significant conformational change in the N-terminal segment producing a reduction in the axial ratio of cTnI and a more compact structure (*32, 47, 48*). These conformational changes weaken the interactions between the N-terminal segment of cTnI and the N-domain of cTnC. A recent NMR and modeling study has suggested that the bisphosphorylated N-terminal segment of cTnI interacts with its inhibitory region through electrostatic interactions (*49*). This suggestion supports the notion that the bisphosphorylation modulates the interactions between the inhibitory region of cTnI and actin−tropomyosin. The observed increases in the FRET distances between cTnI(131) and actin induced by bisphosphorylation are in accord with the NMR and modeling results. The effect of bisphosphorylation on the distances from actin to the other three cTnI sites is not on the magnitude of the distances but on the half-width of the distance distributions. The reduced half-widths are correlated with decreases in structural dynamics of cTnI in the interface between troponin and the actin filament. These results suggest that PKA phosphorylation of cTnI has minimal structural effects, but they may have significant structural dynamic and kinetic effects on cTnI−actin interaction to modulate myofilament Ca^{2+} sensitivity and cross-bridge kinetics.

In summary, we investigated the effects of bound regulatory Ca^{2+}, strongly bound myosin, and PKA bisphosphorylation of cTnI on the distance changes from actin Cys374 to several actin-binding sites within the inhibitory region, regulatory region, and the second actin-binding region of cTnI. The results show that bound Ca^{2+} induces large increases in the distances from actin to the cTnI sites, indicating a Ca^{2+}-triggered separation of cTnI from actin. Bound myosin S1 (S1•MgADP) induces additional increases in these distances. These two ligand-induced increases in the distances between cTnI and actin are independent of each other, and the results provide direct evidence to link structural changes at the interface between cTnI and actin to the three-state model of thin filament regulation of muscle contraction and relaxation. The FRET distance distribution analysis suggests that the second actin-binding region of cTnI within the thin filament is rigid comparing with the inhibitory/regulatory region. The inhibitory region is more flexible in the Ca^{2+}-bound state than in the Mg^{2+} state. PKA phosphorylation of cTnI changes the interaction between actin and the inhibitory region of cTnI. The bisphosphorylation also alters the flexibility of both the inhibitory and regulatory regions of cTnI. These alterations may be related to changes in the electrostatic interactions between the N-terminal segment and the inhibitory region of cTnI.

REFERENCES

1. Ebashi, S., Endo, M., and Otsuki, I. (1969) Control of muscle contraction. *Q. Rev. Biophys. 2*, 351–384.
2. Farah, C. S., and Reinach, F. C. (1995) The troponin complex and regulation of muscle contraction. *FASEB J. 9*, 755–767.
3. Gordon, A. M., Homsher, E., and Regnier, M. (2000) Regulation of contraction in striated muscle. *Physiol. Rev. 80*, 853–924.
4. Kobayashi, T., Jin, L., and de Tombe, P. P. (2008)Cardiac thin filament regulation, *Pfluegers Arch. on-line* (DOI: 10.1007/s00424-008-0511-8).
5. Ohtsuki, I., and Morimoto, S. (2008) Troponin: regulatory function and disorders. *Biochem. Biophys. Res. Commun. 369*, 62–73.
6. Solaro, R. J. (2002) Modulation of cardiac myofilament activity by protein phosphorylation, in *Handbook of Physiology. Section 2: The Cardiovascular System. Volume I: The Heart* (Page, E. F., Harry, A., and Solaro, R. J., Eds.) pp 264−300, Oxford University Press, Oxford.
7. Tobacman, L. S. (1996) Thin filament-mediated regulation of cardiac contraction. *Annu. Rev. Physiol. 58*, 447–481.
8. Dong, W. J., Xing, J., Villain, M., Hellinger, M., Robinson, J. M., Chandra, M., Solaro, R. J., Umeda, P. K., and Cheung, H. C. (1999) Conformation of the regulatory domain of cardiac muscle troponin C in its complex with cardiac troponin I. *J. Biol. Chem. 274*, 31382–31390.
9. Dong, W. J., Chandra, M., Xing, J., Solaro, R. J., and Cheung, H. C. (1997) Conformation of the N-terminal segment of a monocysteine mutant of troponin I from cardiac muscle. *Biochemistry 36*, 6745–6753.
10. Dong, W. J., Xing, J., Robinson, J. M., and Cheung, H. C. (2001) Ca^{2+} induces an extended conformation of the inhibitory region of troponin I in cardiac muscle troponin. *J. Mol. Biol. 314*, 51–61.
11. Smillie, L. B. (1982) Preperation and identification of a- and b-Tropomyosins. *Methods Enzymol. 85*, 234–241.
12. Pardee, J. D., and Spudich, J. A. (1982) Purification of muscle actin. *Methods Enzymol. 85*, 164–181.
13. Xing, J., and Cheung, H. C. (1994) Vanadate-induced changes in myosin subfragment-1 from cardiac muscle. *Arch. Biochem. Biophys. 313*, 229–234.
14. Kobayashi, T., Kobayashi, M., and Collins, J. H. (2001) Ca^{2+}-dependent, myosin subfragment 1-induced proximity changes between actin and the inhibitory region of troponin I. *Biochim. Biophys. Acta 1549*, 148–154.
15. Tao, T., Gong, B. J., and Leavis, P. C. (1990) Calcium-induced movement of troponin-I relative to actin in skeletal muscle thin filaments. *Science 247*, 1339–1341.
16. Robinson, J. M., Dong, W. J., Xing, J., and Cheung, H. C. (2004) Switching of troponin I: Ca(2+) and myosin-induced activation of heart muscle. *J. Mol. Biol. 340*, 295–305.
17. Finley, N., Abbott, M. B., Abusamhadneh, E., Gaponenko, V., Dong, W., Gasmi-Seabrook, G., Howarth, J. W., Rance, M., Solaro, R. J., Cheung, H. C., and Rosevear, P. R. (1999) NMR analysis of cardiac troponin C-troponin I complexes: effects of phosphorylation. *FEBS Lett. 453*, 107–112.
18. Dong, W. J., Xing, J., Chandra, M., Solaro, J., and Cheung, H. C. (2000) Structural mapping of single cysteine mutants of cardiac troponin I. *Proteins 41*, 438–447.
19. Wang, C. K., and Cheung, H. C. (1986) Proximity relationship in the binary complex formed between troponin I and troponin C. *J. Mol. Biol. 191*, 509–521.
20. She, M., Dong, W. J., Umeda, P. K., and Cheung, H. C. (1997) Time-resolved fluorescence study of the single tryptophans of engineered skeletal muscle troponin C. *Biophys. J. 73*, 1042–1055.
21. She, M., Xing, J., Dong, W. J., Umeda, P. K., and Cheung, H. C. (1998) Calcium binding to the regulatory domain of skeletal muscle troponin C induces a highly constrained open conformation. *J. Mol. Biol. 281*, 445–452.
22. Lakowicz, J. R., Gryczynski, I., Cheung, H. C., Wang, C. K., Johnson, M. L., and Joshi, N. (1988) Distance distributions in proteins recovered by using frequency-domain fluorometry. Applications to troponin I and its complex with troponin C. *Biochemistry 27*, 9149–9160.
23. Robinson, J. M., Wang, Y., Kerrick, W. G., Kawai, R., and Cheung, H. C. (2002) Activation of striated muscle: nearest-neighbor regulatory-unit and cross-bridge influence on myofilament kinetics. *J. Mol. Biol. 322*, 1065–1088.
24. Bevington, P. R., and Robinson, D. K. (1992) *Data Reduction and Error Analysis for the Physical Sciences*, 2nd ed., McGraw-Hill, Boston.
25. Cheung, H. C., Wang, C. K., Gryczynski, I., Wiczk, W., Laczko, G., Johnson, M. L., and Lakowicz, J. R. (1991) Distance distributions and anisotropy decays of troponin C and its complex with troponin I. *Biochemistry 30*, 5238–5247.
26. Takeda, S., Yamashita, A., Maeda, K., and Maeda, Y. (2003) Structure of the core domain of human cardiac troponin in the Ca(2+)-saturated form. *Nature 424*, 35–41.
27. Murakami, K., Yumoto, F., Ohki, S. Y., Yasunaga, T., Tanokura, M., and Wakabayashi, T. (2005) Structural basis for Ca^{2+}-regulated muscle relaxation at interaction sites of troponin with actin and tropomyosin. *J. Mol. Biol. 352*, 178–201.
28. Galinska-Rakoczy, A., Engel, P., Xu, C., Jung, H., Craig, R., Tobacman, L. S., and Lehman, W. (2008) Structural basis for the regulation of muscle contraction by troponin and tropomyosin. *J. Mol. Biol. 379*, 929–935.

29. Robinson, J. M., Dong, W. J., and Cheung, H. C. (2003) Can Forster resonance energy transfer measurements uniquely position troponin residues on the actin filament? A case study in multiple-acceptor FRET. *J. Mol. Biol. 329*, 371–380.
30. Pirani, A., Vinogradova, M. V., Curmi, P. M., King, W. A., Fletterick, R. J., Craig, R., Tobacman, L. S., Xu, C., Hatch, V., and Lehman, W. (2006) An atomic model of the thin filament in the relaxed and Ca^{2+}-activated states. *J. Mol. Biol. 357*, 707–717.
31. Sweeney, H. L., Brito, R. M., Rosevear, P. R., and Putkey, J. A. (1990) The low-affinity Ca(2+)-binding sites in cardiac/slow skeletal muscle troponin C perform distinct functions: site I alone cannot trigger contraction. *Proc. Natl. Acad. Sci. U.S.A. 87*, 9538–9542.
32. Dong, W. J., Chandra, M., Xing, J., She, M., Solaro, R. J., and Cheung, H. C. (1997) Phosphorylation-induced distance change in a cardiac muscle troponin I mutant. *Biochemistry 36*, 6754–6761.
33. Sugimoto, Y., Takezawa, Y., Matsuo, T., Ueno, Y., Minakata, S., Tanaka, H., and Wakabayashi, K. (2008) Structural changes of the regulatory proteins bound to the thin filaments in skeletal muscle contraction by X-ray fiber diffraction. *Biochem. Biophys. Res. Commun. 369*, 100–108.
34. Dong, W. J., Robinson, J. M., Stagg, S., Xing, J., and Cheung, H. C. (2003) Ca^{2+}-induced conformational transition in the inhibitory and regulatory regions of cardiac troponin I. *J. Biol. Chem. 278*, 8686–8692.
35. Kobayashi, T., and Solaro, R. J. (2005) Calcium, thin filaments, and the integrative biology of cardiac contractility. *Annu. Rev. Physiol. 67*, 39–67.
36. Li, M. X., Wang, X., and Sykes, B. D. (2004) Structural based insights into the role of troponin in cardiac muscle pathophysiology. *J. Muscle Res. Cell Motil. 25*, 559–579.
37. Maytum, R., Lehrer, S. S., and Geeves, M. A. (1999) Cooperativity and switching within the three-state model of muscle regulation. *Biochemistry 38*, 1102–1110.
38. McKillop, D. F., and Geeves, M. A. (1993) Regulation of the interaction between actin and myosin subfragment 1: evidence for three states of the thin filament. *Biophys. J. 65*, 693–701.
39. Shitaka, Y., Kimura, C., Iio, T., and Miki, M. (2004) Kinetics of the structural transition of muscle thin filaments observed by fluorescence resonance energy transfer. *Biochemistry 43*, 10739–10747.
40. Bremel, R. D., and Weber, A. (1972) Cooperation within actin filament in vertebrate skeletal muscle. *Nat. New Biol. 238*, 97–101.
41. Heeley, D. H., Belknap, B., and White, H. D. (2006) Maximal activation of skeletal muscle thin filaments requires both rigor myosin S1 and calcium. *J. Biol. Chem. 281*, 668–676.
42. Tung, C. S., Wall, M. E., Gallagher, S. C., and Trewhella, J. (2000) A model of troponin-I in complex with troponin-C using hybrid experimental data: the inhibitory region is a beta-hairpin. *Protein Sci. 9*, 1312–1326.
43. Takeda, S., Kobayashi, T., Taniguchi, H., Hayashi, H., and Maeda, Y. (1997) Structural and functional domains of the troponin complex revealed by limited digestion. *Eur. J. Biochem. 246*, 611–617.
44. Hoffman, R. M., Blumenschein, T. M., and Sykes, B. D. (2006) An interplay between protein disorder and structure confers the Ca^{2+} regulation of striated muscle. *J. Mol. Biol. 361*, 625–633.
45. Abbott, M. B., Dong, W. J., Dvoretsky, A., DaGue, B., Caprioli, R. M., Cheung, H. C., and Rosevear, P. R. (2001) Modulation of cardiac troponin C-cardiac troponin I regulatory interactions by the amino-terminus of cardiac troponin I. *Biochemistry 40*, 5992–6001.
46. Gaponenko, V., Abusamhadneh, E., Abbott, M. B., Finley, N., Gasmi-Seabrook, G., Solaro, R. J., Rance, M., and Rosevear, P. R. (1999) Effects of troponin I phosphorylation on conformational exchange in the regulatory domain of cardiac troponin C. *J. Biol. Chem. 274*, 16681–16684.
47. Liao, R., Wang, C. K., and Cheung, H. C. (1994) Coupling of calcium to the interaction of troponin I with troponin C from cardiac muscle. *Biochemistry 33*, 12729–12734.
48. Heller, W. T., Finley, N. L., Dong, W. J., Timmins, P., Cheung, H. C., Rosevear, P. R., and Trewhella, J. (2003) Small-angle neutron scattering with contrast variation reveals spatial relationships between the three subunits in the ternary cardiac troponin complex and the effects of troponin I phosphorylation. *Biochemistry 42*, 7790–7800.
49. Howarth, J. W., Meller, J., Solaro, R. J., Trewhella, J., and Rosevear, P. R. (2007) Phosphorylation-dependent conformational transition of the cardiac specific N-extension of troponin I in cardiac troponin. *J. Mol. Biol. 373*, 706–722.

BI801492X